

# Interleukin 17A Promotes Pneumococcal Clearance by Recruiting Neutrophils and Inducing Apoptosis through a p38 Mitogen-Activated Protein Kinase-Dependent Mechanism in Acute Otitis Media

Wei Wang,<sup>a</sup> Aie Zhou,<sup>b</sup> Xuemei Zhang,<sup>a</sup> Yun Xiang,<sup>a</sup> Yifei Huang,<sup>a</sup> Lei Wang,<sup>a</sup> Shuai Zhang,<sup>a</sup> Yusi Liu,<sup>a</sup> Yibing Yin,<sup>a</sup> Yujuan He<sup>a</sup>

Department of Laboratory Medicine, Key Laboratory of Diagnostic Medicine (Ministry of Education), Chongqing Medical University, Chongqing, People's Republic of China<sup>a</sup>; Department of Laboratory Medicine, Chongqing Traditional Chinese Medicine Hospital, Chongqing, People's Republic of China<sup>b</sup>

*Streptococcus pneumoniae* is a Gram-positive and human-restricted pathogen colonizing the nasopharynx with an absence of clinical symptoms as well as a major pathogen causing otitis media (OM), one of the most common childhood infections. Upon bacterial infection, neutrophils are rapidly activated and recruited to the infected site, acting as the frontline defender against emerging microbial pathogens via different ways. Evidence shows that interleukin 17A (IL-17A), a neutrophil-inducing factor, plays important roles in the immune responses in several diseases. However, its function in response to *S. pneumoniae* OM remains unclear. In this study, the function of IL-17A in response to *S. pneumoniae* OM was examined using an *in vivo* model. We developed a model of acute OM (AOM) in C57BL/6 mice and found that neutrophils were the dominant immune cells that infiltrated to the middle ear cavity (MEC) and contributed to bacterial clearance. Using IL-17A knockout (KO) mice, we found that IL-17A boosted neutrophil recruitment to the MEC and afterwards induced apoptosis, which was identified to be conducive to bacterial clearance. In addition, our observation suggested that the p38 mitogen-activated protein kinase (MAPK) signaling pathway was involved in the recruitment and apoptosis of neutrophils mediated by IL-17A. These data support the conclusion that IL-17A contributes to the host immune response against *S. pneumoniae* by promoting neutrophil recruitment and apoptosis through the p38 MAPK signaling pathway.

Acute otitis media (AOM) is the most common bacterial infectious disease in early childhood, with an incidence of 10.85% (709 million cases each year) and with 51% of these cases occurring in children under 5 years of age (1). Although AOM is typically self-limiting, it may lead to important sequelae such as meningitis and permanent hearing loss (2). *Streptococcus pneumoniae* is the most common pathogen, responsible for 19% to 74% of episodes, followed by nontypeable *Haemophilus influenzae* and *Moraxella catarrhalis* (3). Despite recent advances in our understanding of the pathogenesis of *S. pneumoniae* OM, more needs to be learned about the protective role of the host innate immune defense systems during *S. pneumoniae* OM.

As the founding member of the interleukin-17 (IL-17) cytokine family, IL-17A is an essential effector in the host defense against extracellular bacteria and fungi, particularly at mucosal sites. Conventionally, it is considered to be exclusively produced by T helper 17 (Th17) cells, a unique helper T cell subset distinct from Th1 and Th2 cells, but emerging evidence shows that it can also be produced by CD8<sup>+</sup> T cells,  $\gamma\delta$  T cells, NK T cells, neutrophils, epithelial cells, and innate lymphoid cells (ILCs) (4, 5), suggesting that IL-17A can be produced either by adaptive or innate immune cells. Previous studies indicated that IL-17A, as an activator of neutrophils, participates in the host defense against pathogens, through both neutrophil expansion via regulating the expression of granulocyte colony-stimulating factor (G-CSF) and recruitment to sites of inflammation via regulating the expression of CXC chemokines (6–9). Neutrophils are the first immune cells infiltrating to the infected site as well as the main phagocytes responsible for early pathogen clearance. Growing evidence demonstrates that these infiltrating neutrophils, upon bacterial infection,

become activated and then efficiently constrain and kill microbes via phagocytosis, release of granule contents into extracellular space, cytokine secretion, and the formation of neutrophil extracellular traps (10). In our model, we determined that neutrophils are the first immune cells to infiltrate the middle ear cavity (MEC) to boost bacterial clearance. However, further studies are needed to assess the role and the precise molecular mechanism of neutrophils mediated by IL-17A in the host defense against *S. pneumoniae* challenge during AOM.

In our study, we developed a model of AOM following direct transtympanic inoculation with *S. pneumoniae* clinical strain 6B, which is one of the most frequently used serotypes to cause human otitis media (11). The objective of this study is to determine whether and how IL-17A is associated with the host defense against *S. pneumoniae* during AOM.

In this report, we illustrated that IL-17A promoted bacterial clearance by recruiting neutrophils to the MEC and inducing the apoptosis of recruited neutrophils, both of which actions correlate

Received 3 January 2014 Returned for modification 27 January 2014

Accepted 18 March 2014

Published ahead of print 24 March 2014

Editor: L. Pirofski

Address correspondence to Yujuan He, yujuanhe@cqmu.edu.cn.

Supplemental material for this article may be found at <http://dx.doi.org/10.1128/IAI.00006-14>.

Copyright © 2014, American Society for Microbiology. All Rights Reserved.

doi:10.1128/IAI.00006-14

with the activation of p38 mitogen-activated protein kinase (MAPK) phosphorylation.

## MATERIALS AND METHODS

**Bacteria.** *S. pneumoniae* clinical isolate 31207 (serotype 6B) was obtained from the National Center for Medical Culture Collections (CMCC; Beijing, China). The growth conditions and inocula were previously described (12). Briefly, log-phase cultures were prepared by inoculation in C+Y (casein hydrolysate plus yeast extract) medium with *S. pneumoniae* grown overnight on a Columbia CNA agar plate. After 3 h of incubation, the cultures were centrifuged at  $3,500 \times g$  for 20 min, washed twice, and resuspended in sterile pyrogen-free phosphate-buffered saline (PBS) or vehicle. The concentration of *S. pneumoniae* was determined by standard dilution and plate counts.

**Mice.** Four- to six-week-old male or female C57BL/6 mice bred and housed in a specific-pathogen-free environment were purchased from and raised at Chongqing Medical University, Chongqing, China. IL-17A knockout (IL-17A KO) mice on a C57BL/6 background were kindly provided by Zhinan Yin (College of Life Sciences, Nankai University, Tianjin, china) and Richard A. Flavell (Yale University School of Medicine, New Haven, CT). All animal experiments were performed in accordance with the guidelines of the respective ethics committees of Chongqing Medical University.

**Mouse model of AOM.** AOM was induced by direct bilateral transtympanic inoculation of the middle ear, as previously described (13). Briefly, mice were anesthetized by intraperitoneal injection with ketamine hydrochloride (20 mg/kg of body weight) and xylazine (5 mg/kg). AOM was then produced by direct bilateral transtympanic injection of 5  $\mu$ l of a suspension containing  $1 \times 10^7$  to  $1 \times 10^8$  CFU of *S. pneumoniae* in sterile pyrogen-free PBS. In some cases, 5  $\mu$ l of PBS containing recombinant murine IL-17A (rmIL-17A; 2 ng/ml) (BioLegend, San Diego, CA) and  $1 \times 10^7$  to  $1 \times 10^8$  CFU of *S. pneumoniae* were injected. A control cohort of five mice was sham inoculated with 5  $\mu$ l of PBS alone; an additional five mice were used as normal controls without injection. Mice were anesthetized and then sacrificed at designated time points postchallenge. The middle ear space was lavaged six times with 10  $\mu$ l of sterile pyrogen-free PBS containing 5% fetal calf serum (FCS); the wash fluids were aspirated and pooled. Middle ear lavage fluids (MELF) were centrifuged at  $500 \times g$  for 10 min, and single-use aliquots of the MELF were stored at  $-70^\circ\text{C}$ . The cell pellets were washed twice for total RNA extraction or other detections. Following lavage, the middle ear epithelium was harvested by *in situ* lysis with 10  $\mu$ l of lysis buffer from an RNeasy Minikit (Qiagen, Valencia, CA) (14). This process was repeated six times, and the lysates were aspirated and pooled. Total RNA from the middle ear epithelium lysates pooled from six mice at each time point was extracted by using an RNeasy Minikit according to the manufacturer's instructions (Qiagen, Valencia, CA) and stored at  $-80^\circ\text{C}$  until analyzed by real-time PCR.

**Inhibition of the p38 MAPK signaling pathway and caspase activity *in vivo*.** To inhibit the p38 MAPK signaling pathway and caspase activity, the mice were inoculated with *S. pneumoniae* plus the p38 MAPK inhibitor SB-203580 (25  $\mu$ M in PBS; Merck KGaA, Darmstadt, Germany) or the general caspase inhibitor Z-VAD-FMK (carboxybenzyl-Val-Ala-Asp-fluoromethylketone; 50  $\mu$ M in PBS) (R&D Systems, Minneapolis, MN) by direct bilateral transtympanic inoculation of the middle ear, as previously described (13).

**Quantitation of mRNA from the middle ear epithelium and MELF cells by real-time PCR.** Real-time PCR assays were performed to quantitate IL-17A, IL-23p19, and IL-23p40 transcripts. Total RNA from the middle ear epithelium lysate sample was reverse transcribed with random hexamers by using a Superscript preamplification system (Invitrogen, Carlsbad, CA). cDNA was then used for real-time PCR using SYBR green MasterMix (TaKaRa Bio, Inc., Tokyo, JP) on an ABI Prism 7000 (Applied Biosystems, Foster City, CA) with SYBR green I dye as the amplicon detector. The gene for  $\beta$ -actin was amplified as an endogenous reference. Primer and probe sequences were as follows: IL-

17A, 5'-ATCCCTCAAAGCTCAGCGTGTC-3' (sense) and 5'-GGGTCTTCATTGCGGTGGAGAG-3' (antisense); IL-23p40, 5'-ACCTGTGACACGCCTGAAGAAGAT-3' (sense) and 5'-TCTTGTGGAGCAGCAGATGTGAGT-3' (antisense); IL-23p19, 5'-CAACTTCACACCTCCCTAC-3' (sense) and 5'-CCACTGCTGACTAGAACT-3' (antisense);  $\beta$ -actin, 5'-TGGGAATCCTGTGGCATCCATGAAAC-3' (sense) and 5'-TAAACCGCAGCTCAGTAACAGTCCG-3' (antisense).

**Quantitation of cytokines in the MELF by ELISA.** IL-17A in the MELF pooled from six mice was measured by use of commercial enzyme-linked immunosorbent assay (ELISA) kits (Quantikine; R&D Systems, Minneapolis, MN), according to the manufacturer's instructions. Middle ear lavage samples pooled from six sham-inoculated animals served as the controls.

**Flow cytometry.** MELF were pooled from four to five mice as described above, cells were centrifuged at  $500 \times g$ , the cell pellets were washed twice, and then Fc receptors were blocked with Mouse BD Fc Block (BD Biosciences, San Diego, CA). Thereafter, cells were stained with specific immune cell surface markers. The following staining parameters were employed: neutrophils as CD11b<sup>+</sup> Ly-6G<sup>+</sup>, cells in early apoptosis as annexin V positive/propidium iodide negative (annexin V<sup>+</sup>/PI<sup>-</sup>), and cells in late apoptosis as annexin V<sup>+</sup>/PI<sup>+</sup> (all antibodies were purchased from eBiosciences and BD Biosciences). For intracellular IL-17A staining (15, 16), cells were collected, and Fc receptors were blocked (as described above). The cells were first stained with a fluorescein isothiocyanate (FITC)-conjugated anti-mouse Ly-6G and then permeabilized and stained with phycoerythrin (PE)-conjugated IL-17A or an isotype control antibody using a BD Cytofix/Cytoperm fixation/permeabilization solution kit (BD Biosciences, San Diego, CA) according to the manufacturer's instructions. Unstained cells served as a control for background fluorescence and gating. All samples were resuspended in the wash buffer and data were collected by flow cytometry (FACSCalibur; BD Biosciences, San Jose, CA).

**Bacterial load determination.** The mice were sacrificed at designated time points postchallenge. Bacterial loads in MELF of *S. pneumoniae*-infected wild-type (WT) and IL-17A KO mice were determined by plating 10-fold serial dilutions of aliquots from the respective MELF of each mouse on Columbia CNA agar plate. The colonies were counted after overnight incubation at  $37^\circ\text{C}$  in a 5% CO<sub>2</sub> atmosphere. The limit of detection in colonization studies was 10 CFU/animal.

**Cell quantification.** MELF were pooled from four to five mice, and cells were centrifuged at  $500 \times g$ . The cell pellets were washed twice and then resuspended in 500  $\mu$ l of PBS. Cell quantification was performed by counting the cells based on standard morphological criteria at a magnification of  $\times 400$ . The absolute total number of the cells in the middle ear lavage fluids was used for data analysis.

**H&E staining and immunohistochemistry.** Temporal bones from four to five mice in each cohort were removed immediately after sacrifice at designated time points postchallenge. The samples were processed as described previously with minor modifications (12). The middle ear sections were deparaffinized and rehydrated through Histo-Clear and a graded alcohol series. The specimens were further processed for conventional paraffin embedding. Serial sections were cut to a thickness of 6  $\mu$ m and stained with hematoxylin and eosin (H&E). For immunohistochemistry, the endogenous peroxidase activity was blocked with 0.3% H<sub>2</sub>O<sub>2</sub> in 0.1 M phosphate-buffered saline (PBS) (pH 7.4), and the sections were incubated with 0.05% trypsin solution (Invitrogen, Carlsbad, CA) to unmask antigens. The sections were blocked with PBS (pH 7.2) containing 1% bovine serum albumin (BSA), 5% donkey serum, and 0.3% Triton X-100 and then incubated with primary antibodies: rat anti-Bax (B-9) (1:100; Santa Cruz Biotechnology, OR, USA) and rat anti-Bcl-xL (7B2.5) (1:100; Santa Cruz Biotechnology, OR, USA). Secondary antibody, horseradish peroxidase (HRP)-conjugated goat anti-rabbit IgG (Zhongshanjinqiao, Beijing, China), was developed by a diaminobenzidine substrate kit for peroxidase (Zhongshanjinqiao, Beijing, China) and then counterstained with hematoxylin (Zhongshanjinqiao, Beijing, China). For

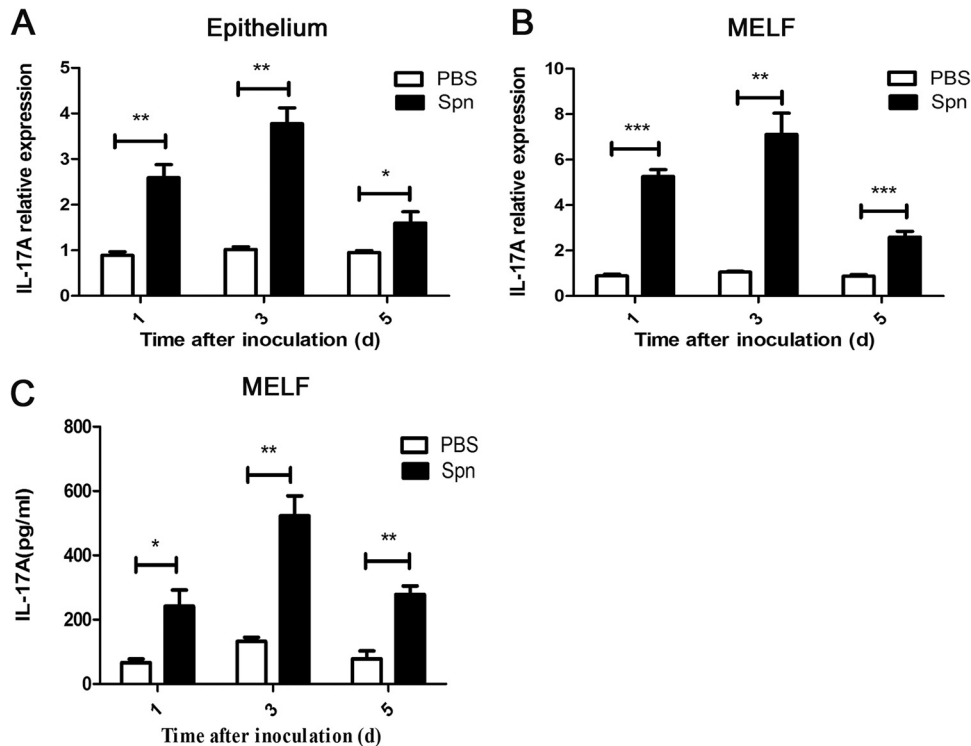


**FIG 1** IL-17A is expressed in response to *S. pneumoniae* during AOM. IL-17A mRNA expression in middle ear epithelium (A) and MELF (B) was analyzed by real-time PCR at designated time points postinfection. Values are expressed as relative gene expression (compared with the level of glyceraldehyde-3-phosphate dehydrogenase). (C) IL-17A levels in the supernatants of MELF were detected by ELISA. Values represent means  $\pm$  SD ( $n = 6$ ). \*,  $P < 0.05$ ; \*\*,  $P < 0.01$ ; \*\*\*,  $P < 0.001$  (between two groups). Cumulative data from three independent studies are shown. Spn, *S. pneumoniae*; d, days.

immunohistochemistry of the cytospin preparation, MELF were pooled from at least three mice as described above. The cell pellets were washed twice and fixed in 2% paraformaldehyde. The cytospin preparations were blocked with PBS with 3% BSA and then incubated with a rabbit polyclonal antibody to pneumococcal polysaccharide (1:1,000; Statens Serum Institute, Copenhagen, Denmark) and rat anti-mouse elastase monoclonal antibody (Mab) (1:100; Cell Sciences, Canton, MA). Secondary antibodies were donkey anti-rabbit IgG coupled with DyLight 594 and donkey anti-rat IgG conjugated with DyLight 488 (1:1,000; Jackson Immuno-Research Laboratories, West Grove, PA). The slides were washed and counterstained with 4',6'-diamidino-2-phenylindole (DAPI; 1:10,000) (Invitrogen, Carlsbad, CA). The samples were mounted with Vectashield mounting medium (Vector Laboratories, Burlingame, CA). Immunostained samples were examined with a Zeiss Axioskop microscope equipped with an Olympus Magnafire low-light color digital camera or with an Olympus FluoView 1000 laser scanning confocal microscope.

**Western blotting.** To evaluate the kinetics of phospho-p38 (p-p38) protein production in epithelium during AOM, epithelial tissues from middle ear samples pooled from four to five mice at designated time points postchallenge were subjected to SDS-PAGE. Samples were transferred to polyvinylidene difluoride (PVDF) membranes. The membranes were blocked and then incubated with rabbit anti-mouse p-p38 antibody (1:1,000; Cell Signaling Technology, MA, USA) or anti- $\beta$ -actin antibody (1:1,000; Cell Signaling Technology, MA, USA) containing 5% BSA. Blots were then washed and incubated with horseradish peroxidase (HRP)-conjugated goat anti-rabbit IgG (1:10,000; Zhongshanjinqiao, Beijing, China) that was developed by an ECL kit (Millipore, Billerica, MA) and diluted in Tris-buffered saline plus Tween (TBST) containing 5% BSA.

**Quantitation of caspase-3 in MELF.** Concentrations of caspase-3 in the MELF pooled from four to five mice were measured by caspase-3 activity assay kits (Beyotime, China), based on the ability of caspases to

change acetyl-Asp-Glu-Val-Asp *p*-nitroanilide into the yellow formazan product *p*-nitroaniline. According to the manufacturer's protocol, cell pellets of MELF were lysed with lysis buffer (100  $\mu$ l per  $2 \times 10^6$  cells) for 15 min on ice, followed by washing with cold PBS. A mixture of 20  $\mu$ l of cell lysate, 70  $\mu$ l of reaction buffer, and 10  $\mu$ l of 2 mM caspases substrate in 96-well microtiter plates was incubated at 37°C for 2 h. The caspase-3 activity was determined at an absorbance of 405 nm. MELF pooled from four sham-inoculated animals served as the controls.

**Statistical analysis.** Data are presented as the means  $\pm$  standard deviations (SD) of three independent experiments. Independent *t* tests were used for data with normal distribution, and Mann-Whitney U tests were performed for data with nonnormal distribution. Statistical significance was set at a *P* value of  $< 0.05$ . All data were analyzed using GraphPad Prism software, version 5.01, for Windows (GraphPad, USA).

## RESULTS

***S. pneumoniae* inducing an increase in gene and protein expression of IL-17A in response to AOM.** AOM was produced by *S. pneumoniae* clinical strain 6B in C57BL/6 mice, and sterile PBS was selected as a sham-inoculated control. Figure 1 displays the expression of IL-17A in responses to *S. pneumoniae* infection during AOM. At days 1, 3, and 5 postinoculation, we observed an increase in IL-17A mRNA expression in middle ear epithelium by real-time PCR. The rising expression level peaked at day 3 and declined gradually thereafter (Fig. 1A). Similar kinetics for IL-17A mRNA expression was seen in the cells of MELF (Fig. 1B). Additionally, we measured the protein level of IL-17A in MELF by ELISA. Compared with the sham-inoculated control, an elevated IL-17A concentration in MELF was detected during the observa-

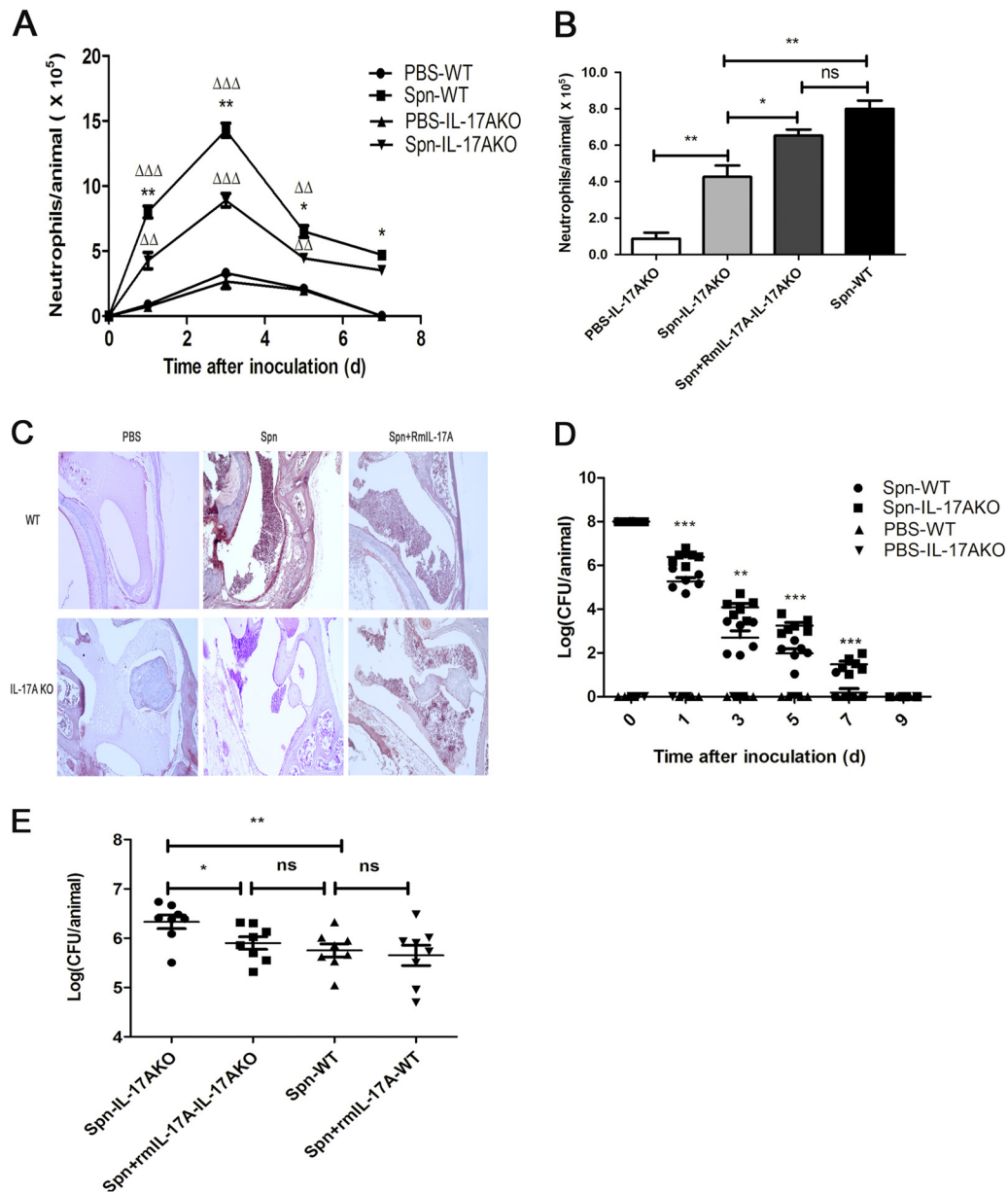


**FIG 2** IL-17A contributes to *S. pneumoniae* clearance by inducing the recruitment of neutrophils during AOM. (A) The absolute numbers of neutrophils in MELF at designated time points postinfection of WT mice and IL-17A KO mice are shown. (B) The absolute numbers of neutrophils in MELF of WT mice and IL-17A KO mice following direct bilateral transtympanic inoculation of *S. pneumoniae* or *S. pneumoniae* plus rmIL-17A at day 1 postinfection are shown. The cells were stained with MAb against neutrophil surface molecules and analyzed by flow cytometry. The ratio of neutrophils (Ly-6G<sup>+</sup> CD11b<sup>+</sup>) was determined, and the absolute number of the cells was calculated. Values represent means  $\pm$  SD ( $n = 4$  to  $5$ ). \*,  $P < 0.05$ ; \*\*,  $P < 0.01$ ; \*\*\*,  $P < 0.001$  (IL-17A KO mice versus WT mice);  $\Delta$ ,  $P < 0.05$ ;  $\Delta\Delta$ ,  $P < 0.01$ ;  $\Delta\Delta\Delta$ ,  $P < 0.001$  (IL-17A KO mice or WT mice versus sham-infected mice). (C) Sections of the middle ear were stained with H&E. Original magnification,  $\times 100$ . (D) Density of *S. pneumoniae* colonization in MELF at designated time points postinfection of WT mice and IL-17A KO mice. Values represent means  $\pm$  SD ( $n = 6$ ). \*,  $P < 0.05$ ; \*\*,  $P < 0.01$ ; \*\*\*,  $P < 0.001$  (IL-17A KO mice versus WT mice). (E) Density of *S. pneumoniae* colonization in MELF at day 1 following direct bilateral transtympanic inoculation of *S. pneumoniae* or *S. pneumoniae* given with rmIL-17A in WT mice or IL-17A KO mice. Values represent means  $\pm$  SD ( $n = 6$ ). \*,  $P < 0.05$ ; \*\*,  $P < 0.01$  (between two groups). Data representative of three independent experiments are demonstrated in all the panels.

tion period, showing consistency with the result of mRNA expression (Fig. 1C). Since IL-23 is known to be a cytokine required for production and maintenance of IL-17A (17), we examined the mRNA expression of IL-23p19 and p40, the two subunits of the IL-23 dimer, and found that both of them were dramatically increased both in middle ear epithelium and in MELF compared to

levels in the controls (see Fig. S1 in the supplemental material). Thus, we concluded that IL-17A is the effector in response to *S. pneumoniae* in AOM.

**IL-17A contributes to bacterial clearance by inducing neutrophil recruitment during AOM.** AOM was produced with *S. pneumoniae* 6B in IL-17A KO mice, as in C57BL/6 mice. To de-

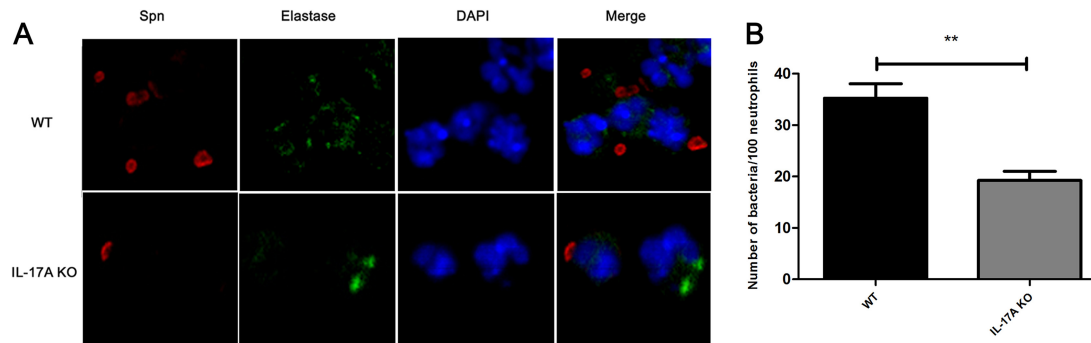


**FIG 3** Confocal microscope images of opsonophagocytosis of *S. pneumoniae* by neutrophils in the cytospin preparations of MELF from WT and IL-17A KO mice. (A) These cytospin preparations were immunofluorescently labeled to visualize *S. pneumoniae* (red), elastase (green), and nucleic acids (blue). Original magnification,  $\times 1,000$ . (B) The number of bacteria phagocytosed by neutrophils in MELF. The absolute numbers of bacteria phagocytosed by neutrophils in MELF of WT mice and IL-17A KO mice following direct bilateral transtympanic inoculation of *S. pneumoniae* at day 3 postinfection are shown. Quantification of the number of bacteria was obtained from at least 20 fields of each section. Values represent means  $\pm$  SD of 4 to 5 animals per group. \*\*,  $P < 0.01$  (between two groups).

to determine the role of IL-17A in AOM, we first conducted a quantitative analysis of immune cells in MELF by flow cytometry. Cumulative data showed that more than 98% of MELF cells, pooled from six mice per time point from WT or IL-17A KO mice, were neutrophils ( $CD11b^+ Ly-6G^+$  cells) (see Fig. S2 in the supplemental material), about 69% of which could produce IL-17A (see Fig. S3). Similarly, Wright's-Giemsa staining of the cytospin preparations showed that more than 98% of the MELF cells were neutrophils, too (see Fig. S4). As expected, the cell quantification of MELF exhibited a significant decrease in neutrophils recruited to the MEC in IL-17A KO mice compared with levels in WT mice (Fig. 2A). Inoculation with *S. pneumoniae* plus exogenous recombinant murine IL-17A (rmIL-17A) restored the ability of IL-17A KO mice to recruit neutrophils in contrast to mice inoculated with *S. pneumoniae* plus vehicle alone (Fig. 2B). In accordance, we obtained the same results by hematoxylin and eosin (H&E) staining of histologic sections as by cell quantification of MELF (Fig. 2C). These findings demonstrated that the early immune cells in response to *S. pneumoniae* AOM were neutrophils in both WT mice and IL-17A KO mice, but the recruitment of neutrophils abated in IL-17A KO mice, which suggests that IL-17A was the effector contributing to migration and recruitment of neutrophils.

Next, we examined bacterial burden in the MELF and found that the density of *S. pneumoniae* decreased gradually over the observation period. It was worth noting that the MELF IL-17A KO mice had 10- to 100-fold more CFU than WT mice (Fig. 2D). The eventual clearance of the bacteria occurred at day 7 in WT mice, while it occurred in IL-17A KO mice later, at day 9 (Fig. 2D). Nevertheless, the delay could be recovered by the administration of rmIL-17A (Fig. 2E). The experiment results suggested that the delay in bacterial clearance was associated with the diminished recruitment of neutrophils. In addition, confocal microscopy showed that the neutrophils in the MELF of WT mice exhibited a stronger phagocytic capability than those of IL-17A KO mice (Fig. 3A and B). The evidence showed that IL-17A facilitates the clearance of *S. pneumoniae* by inducing the recruitment of neutrophils.

**IL-17A induces neutrophil recruitment through the p38 MAPK signaling pathway during AOM.** To further elucidate the mechanism by which IL-17A promotes neutrophil recruitment against *S. pneumoniae* challenge during AOM, we investigated the downstream signaling pathway for IL-17A. Specifically, by West-

ern blotting, we detected a higher phosphorylation level of p38 MAPK in middle ear epithelial cells of WT mice than in the PBS control cohort at days 1, 3, and 5 postchallenge (Fig. 4A). At the same time, we saw a lower phosphorylation level of p38 MAPK in IL-17A KO mice than in WT mice. After the administration of rmIL-17A, the phosphorylation level of p38 MAPK in IL-17A KO mice was partially recovered (Fig. 4B). These findings suggested that IL-17A contributed to the activation of the p38 MAPK signaling pathway. On the other hand, after administering p38 MAPK inhibitor SB-203580 (see Fig. S5 in the supplemental material), we observed reduced neutrophil recruitment and subsequently impaired bacterial clearance in MELF from WT mice and IL-17A KO mice, respectively (Fig. 4C and D), suggesting that p38 MAPK contributed to bacterial clearance by neutrophil recruitment.

Taking these results together, our study demonstrated that neutrophil recruitment induced by IL-17A is highly associated with the p38 MAPK signaling pathway and thereby facilitates bacterial clearance in *S. pneumoniae* AOM.

**IL-17A contributes to bacterial clearance by inducing neutrophil apoptosis during AOM.** Our preliminary research has demonstrated that the infiltrating neutrophils of MELF exhibited typical apoptosis characteristics (data not shown), leading to the hypothesis that neutrophil apoptosis is possibly involved in the immune response against *S. pneumoniae* challenge during AOM. Thus, we examined the kinetics of neutrophil apoptosis by flow cytometry, in which annexin V<sup>+</sup>/PI<sup>-</sup> cells represent early apoptotic cells and annexin V<sup>+</sup>/PI<sup>+</sup> cells represent late apoptotic/necrotic cells. The results showed that neutrophils in MELF from WT mice underwent apoptosis after *S. pneumoniae* inoculation, whereas IL-17A KO mice exhibited a significantly reduced apoptosis rate (Fig. 5A). In accordance, middle ear tissue histologic sections of IL-17A KO mice revealed a lower level of the proapoptotic protein BAX and a higher level of the antiapoptotic protein Bcl-xL in neutrophils than in WT mice (Fig. 5B and C). Furthermore, neutrophils in MELF from IL-17A KO mice showed inhibited caspase-3 activation (Fig. 5D), while their apoptosis was repaired by the administration of rmIL-17a (Fig. 5F), suggesting that IL-17A is involved in neutrophil apoptosis. In addition, after administering Z-VAD-FMK (a general caspase inhibitor) in WT mice (see Fig. S6 in the supplemental material), we found a significant rise of bacterial burden in MELF

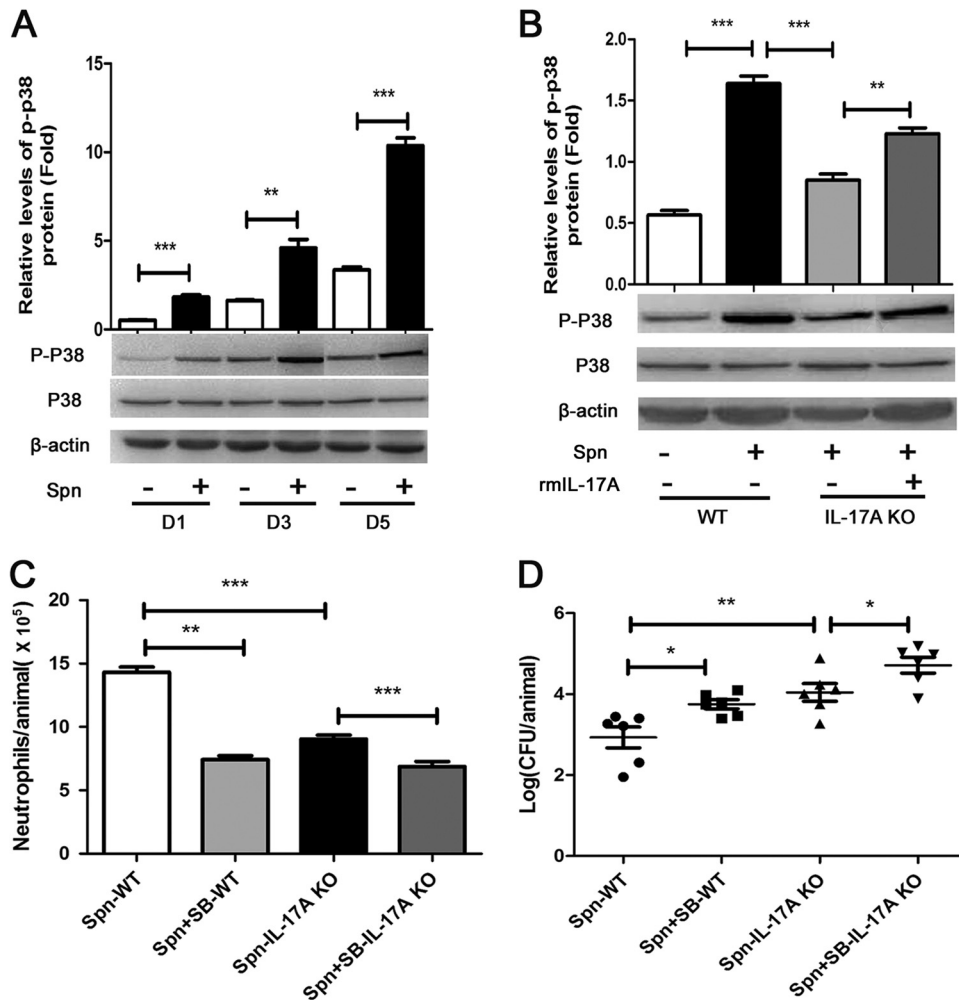


**FIG 4** IL-17A induces neutrophil recruitment through the p38 MAPK signaling pathway during AOM. (A) The total proteins of epithelium in the middle ear of WT mice were extracted, and p-p38 was analyzed by Western blotting at designated times postinfection. D, day. (B) p-p38 protein of WT mice or IL-17A KO mice following direct bilateral transtympanic inoculation of *S. pneumoniae* or *S. pneumoniae* plus rmIL-17A at day 1 postinfection was analyzed by Western blotting. Histograms represent densitometric analysis. The relative values of p-p38 to total protein were calibrated with  $\beta$ -actin. Values represent means  $\pm$  SD ( $n = 4$  to 5). \*\*,  $P < 0.01$ ; \*\*\*,  $P < 0.001$  (between two groups). The absolute numbers of neutrophils (C) and density of *S. pneumoniae* colonization (D) in MELF of WT and IL-17A KO mice following direct bilateral transtympanic inoculation of *S. pneumoniae* or *S. pneumoniae* plus SB-203580 (SB) (a p38 MAPK-specific inhibitor) at day 3 postinfection were analyzed. Values represent means  $\pm$  SD ( $n = 4$  to 6). \*,  $P < 0.05$ ; \*\*,  $P < 0.01$  (between two groups). Data representative of three independent experiments are demonstrated in all the panels.

(Fig. 5E), compared with that of the vehicle cohort, suggesting that neutrophil apoptosis, a host protection mechanism, contributes to *S. pneumoniae* clearance during AOM.

**IL-17A induces neutrophil apoptosis through the p38 MAPK signaling pathway during AOM.** Employing a p38 MAPK signaling pathway inhibitor (SB-203580) in our model, we found a remarkable decline in the apoptosis rate of neutrophils as well as the activity of caspase-3 in MELF (Fig. 6A and B), indicating the involvement of the p38 MAPK signaling pathway in neutrophil apoptosis during AOM. In short, our data showed that IL-17A induces the apoptosis of neutrophils through the p38 MAPK signaling pathway and thereby facilitates the clearance of *S. pneumoniae* during AOM.

## DISCUSSION

AOM is the second most common infectious childhood disease. If improperly treated, AOM can develop into chronic OM, causing

hearing impairment. More serious complications could include deafness and language and intellectual disabilities. The mechanism of the host immune response against *S. pneumoniae* AOM remains largely unknown. To explore it, we developed a model of AOM in C57BL/6 mice using *S. pneumoniae* clinical strain 6B. Our study showed that IL-17A contributes to *S. pneumoniae* clearance in AOM by inducing the recruitment and apoptosis of neutrophils through the p38 MAPK signaling pathway.

As the most populous of immune cells, neutrophils serve as the first defense line against pathogen invasion (18). It is generally believed that neutrophils play a critical role in the host immune response against Gram-positive bacteria. With *S. pneumoniae* infection, neutrophils are the earliest effector cells recruited to the infected site, whether in asymptomatic nasopharynx colonization or invasive lung infection. With neutrophil depletion, the *S. pneumoniae* colonization will develop into an invasive infection, indi-

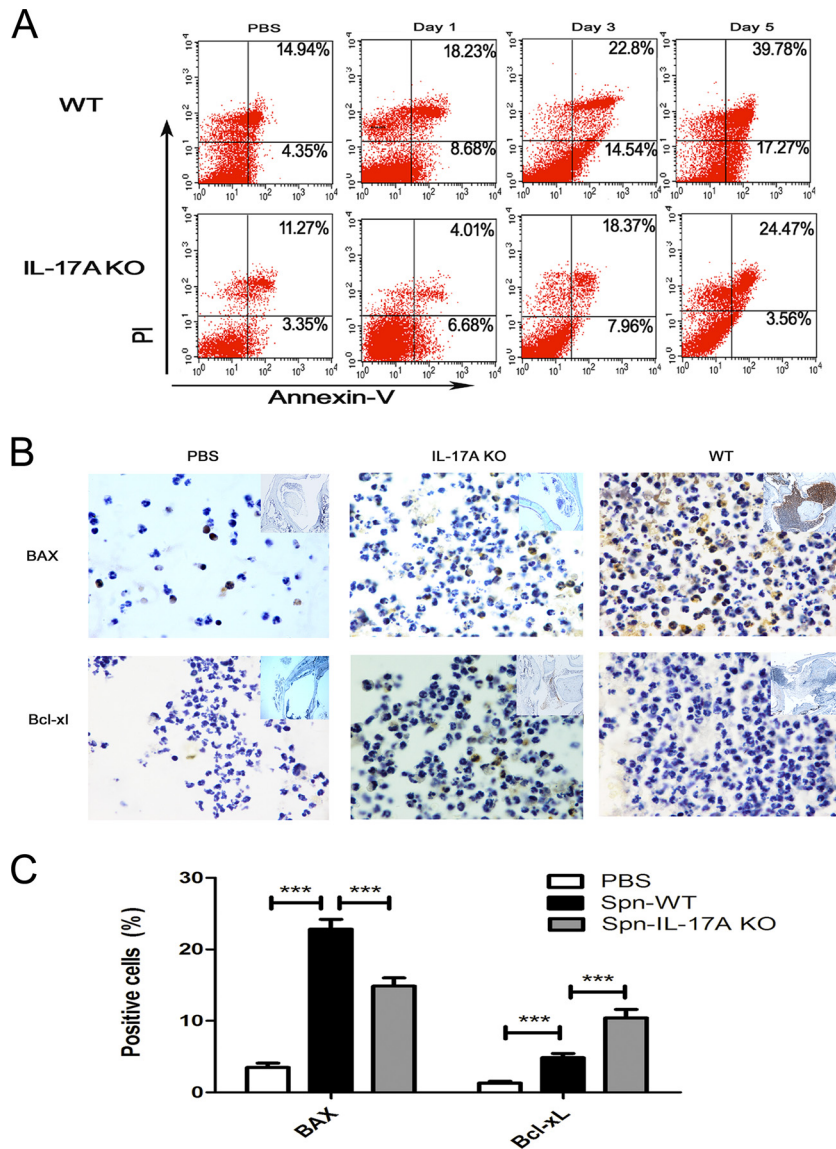


**FIG 5** IL-17A contributes to bacterial clearance by inducing neutrophil apoptosis. (A) Representative dot plots to show the percentage of neutrophil apoptosis by flow cytometry ( $n = 4$  to 5). (B) Representative photomicrographs of immune-histochemistry staining of BAX and Bcl-xL of middle ear sections of WT mice and IL-17A KO mice at day 3 postinfection ( $n = 4$  to 5). Original magnification,  $\times 1,000$ . (C) The percentage of neutrophils expressing BAX and Bcl-xL in middle ear tissue histologic sections of WT mice and IL-17A KO mice at day 3 postinfection. Quantification of the positive neutrophils and total neutrophils was obtained from at least 20 fields of each middle ear section. Values represent means  $\pm$  SD of 4 to 5 animals per group. \*\*\*,  $P < 0.001$  (between two groups). (D) Fold change of caspase-3 activation in MELF of WT and IL-17A KO mice inoculated with *S. pneumoniae* relative to that in inoculation with PBS at the time indicated. Values represent means  $\pm$  SD ( $n = 4$  to 5). \*,  $P < 0.05$ ; \*\*,  $P < 0.01$ ; \*\*\*,  $P < 0.001$  (between two groups). (E) Density of *S. pneumoniae* colonization in MELF of WT mice was analyzed following direct bilateral transtympanic inoculation of *S. pneumoniae* or *S. pneumoniae* plus Z-VAD-FMK (a general caspase inhibitor) at day 3 postinfection. Values represent means  $\pm$  SD ( $n = 6$ ). \*,  $P < 0.05$ ; \*\*,  $P < 0.01$ ; \*\*\*,  $P < 0.001$  (between two groups). (F) The percentage of neutrophil apoptosis in MELF of WT or IL-17A KO mice following direct bilateral transtympanic inoculation of *S. pneumoniae* or *S. pneumoniae* plus rmIL-17A at day 1 postinfection ( $n = 4$  to 5). Data representative of three independent experiments are demonstrated in all the panels.

cating the importance of neutrophils in control of *S. pneumoniae* infection (19). In support of this view, we found that more than 98% of effector cells recruited firstly in the AOM model were neutrophils; this level peaked at day 3 and declined gradually thereafter.

IL-17A, a cytokine, is generally considered to be responsible for governing both neutrophil- and macrophage-characterized inflammation. It has been suggested that IL-17 is produced systemically while it exerts proinflammatory effects locally through reg-

ulation of epithelial cells that are able to express a broad spectrum of chemokines that recruit immune effector cells, including neutrophils and macrophage precursor cells (4, 20, 21).

Our study observed increased expression of IL-17A after *S. pneumoniae* challenge. In accordance with the view that IL-23 is a cytokine necessary for the production of IL-17A, we detected remarkable upregulation of IL-23p19 and p40 mRNA expression in both middle ear epithelium and MELF from infected cohorts (22). Furthermore, given that IL-6 and tumor necrosis factor alpha

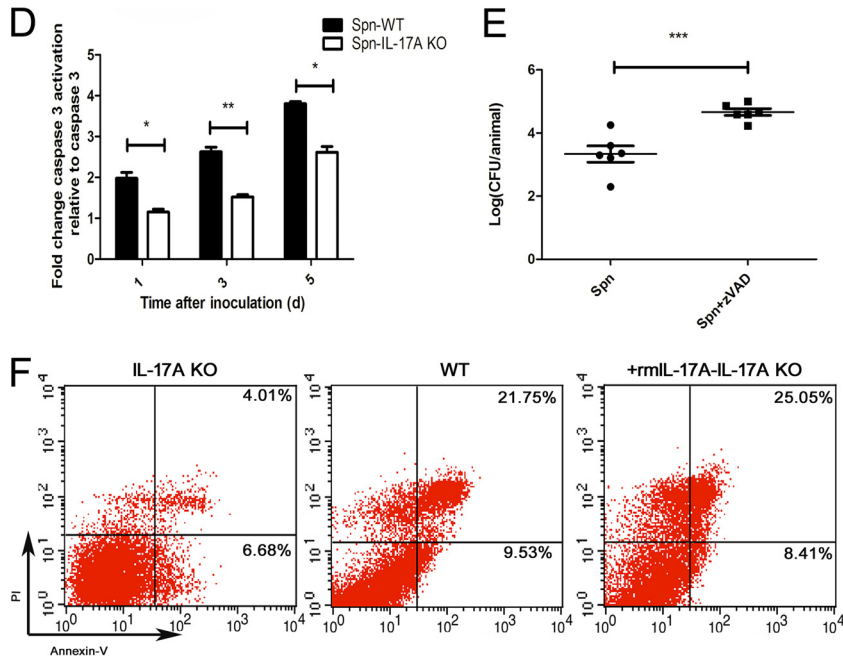


FIG 5 continued

(TNF- $\alpha$ ) are also confirmed to be the key cytokines for the production and maintenance of IL-17A (23–25), we observed increased expression of IL-6 and TNF- $\alpha$ , adding further weight to that view. The high-level expression of IL-17A in AOM suggested that IL-17A was possibly involved in the host immune response in our model. Compared to WT mice, the recruited neutrophils and the bacterial burden in MEC of IL-17A KO mice were found to undergo decrease and increase, respectively, before levels were partially restored to normal with the administration of rmIL-17A. These results provided evidence that IL-17A promotes *S. pneumoniae* clearance by inducing the recruitment of neutrophils in AOM. However, there might have been other factors contributing to neutrophil recruitment and bacterial clearance during *S. pneumoniae* AOM, such as cytokines (IL-1 $\beta$ , TNF- $\alpha$ , etc.) and chemokine ligands (CXCL-8, CXCL-1, etc.), which have been verified in other instances of acute inflammation (26).

Prior research has confirmed that signaling pathways, such as extracellular signal-regulated kinase (ERK), p38 MAPKs, and phosphatidylinositol 3-kinase (PI3K)-Akt, are involved in the recruitment of leukocytes in both the pneumonia and gastritis models (27). Particularly, the p38 MAPK signaling pathway is closely related to inflammation as well as growth, differentiation, and cell death (28). The mitogen-activated protein kinase (MAPK) family, mainly composed of three members, including Jun N-terminal protein kinase (JNK), ERK, and p38 MAPK, is fundamental in mediating a series of inflammatory responses, such as cytokine expression, proliferation, and apoptosis (29, 30). The interaction between p38 MAPK and IL-17A has been confirmed to be important in the immune response (31, 32). For example, by activating p38 MAPK pathways in ARPE-19 (where ARPE is acute retinal pigment epitheliitis) cells, IL-17A can bring about a high level of proinflammatory cytokine production (30). In our study, IL-17A

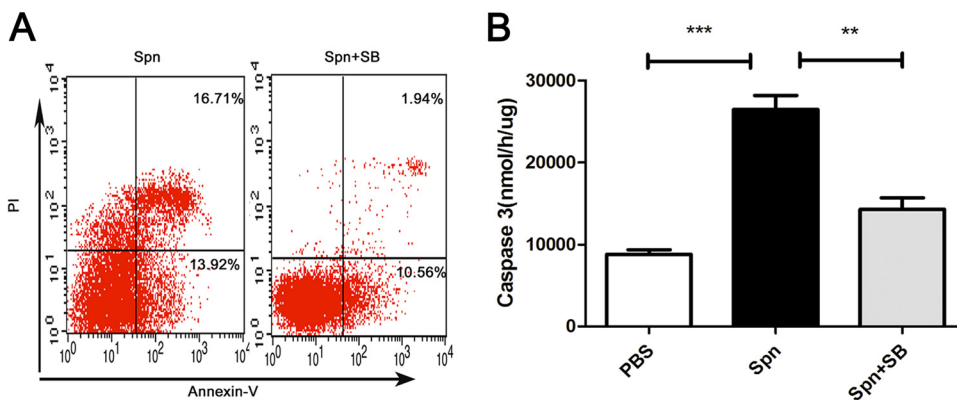


FIG 6 IL-17A induces neutrophil apoptosis through the p38 MAPK signaling pathway during AOM. The percentage of neutrophils in apoptosis (A) and caspase-3 activation (B) in MELF of WT mice following direct bilateral transtympanic inoculation of *S. pneumoniae* or *S. pneumoniae* plus SB-203580 (a p38 MAPK-specific inhibitor) at day 3 postinfection. Values represent means  $\pm$  SD ( $n = 4$  to 5). \*\*,  $P < 0.01$ ; \*\*\*,  $P < 0.001$  (between two groups).



KO mice exhibited a lower level of p38 MAPK phosphorylation in epithelia than WT mice and then recovered with the addition of rmIL-17A. These data indicated that the recruitment of neutrophils induced by IL-17A is related to the p38 MAPK signaling pathway. On the other hand, after administering the p38 MAPK inhibitor SB-203580, we observed impaired neutrophil recruitment as well as enhanced bacterial burden in MELF whether in WT mice or IL-17A KO mice. This result suggested the existence of an IL-17A-independent mechanism which activates the p38 MAPK signaling pathway to regulate neutrophil recruitment and bacterial clearance. In addition, considering that ERK might also be involved in the immune response, we measured the level of the ERK signaling pathway after *S. pneumoniae* inoculation and found its activation in both WT and IL-17A KO mice in comparison with the control cohort, but we did not see a significant difference between the WT and IL-17A KO mice in three independent experiments (data not shown). These results suggested that IL-17A is not associated with the ERK signaling pathway. So it was possibly factors other than IL-17A, we estimated, that activated ERK signaling in our *S. pneumoniae* AOM model.

To fight pathogen invasion, neutrophils induce the generation of reactive oxygen species (ROS) and release of cytotoxic granule components into phagocytic vacuoles to kill phagocytosed pathogens. Conversely, these phagocytosed pathogens were shown to have an impact on neutrophil viability, e.g., apoptosis, autophagy, and survival (33). Apoptosis was first described as a survival strategy of intracellular pathogens that facilitates immune evasion (34, 35). However, recent studies show that macrophage apoptosis is linked to microbial killing (36), while abated macrophage apoptosis leads to a higher rate of invasive pneumococcal disease (37). Additionally, in pneumococcal pneumonia, the macrophage apoptosis induced by TNF-related apoptosis-inducing ligand (TRAIL) was found to directly participate in the killing of *S. pneumoniae* (38). Furthermore, caspase inhibition of macrophage apoptosis also weakens bacterial killing of monocyte-derived macrophage (39). The neutrophil, a phagocyte with high mobility, responsively migrates to the infected site to fight against microbial pathogens. Meanwhile, it likely undergoes apoptosis after phagocytosis of microorganisms (40). In accordance, our study observed the apoptosis of neutrophils in the wake of phagocytosis of pathogens after *S. pneumoniae* inoculation. Notably, neutrophil apoptosis in MELF from IL-17A KO mice showed a remarkable decline before recovery with the supplementation of IL-17A, suggesting that IL-17A facilitates the process of neutrophil apoptosis. Thus, in short, IL-17A, as the neutrophil-inducing factor, keeps recruiting neutrophils to the infected site as well as inducing the apoptosis of recruited neutrophils to maintain the balance of the inflammatory response. Additionally, we observed significantly increased bacterial burden in MELF after administering Z-VAD-FMK (a general caspase inhibitor), indicating the role of neutrophil apoptosis in bacterial clearance. It is reported that p38 MAPK was preferentially activated by cell stress-inducing signals (e.g., oxidative stress) and involved in the proapoptotic pathway in response to several stresses (41, 42). In consistency with the view that the p38 MAPK signaling pathway is related to neutrophil apoptosis, we detected significantly reduced neutrophil apoptosis after administration of the p38 MAPK inhibitor SB-203580. The above data indicated that IL-17A contributes to the *S. pneumoniae* clearance

in AOM by inducing the recruitment and apoptosis of neutrophils through the p38 MAPK signaling pathway.

In conclusion, our study confirmed that IL-17A, as the first line of the immune response, plays a significant role in the process of *S. pneumoniae* clearance. Specifically, IL-17A promotes *S. pneumoniae* clearance by inducing the recruitment and apoptosis of neutrophils through the p38 MAPK signaling pathway. At the same time, we have noticed that IL-17A contributed to tissue damage, and the study of its mechanism is undergoing. Further studies focusing on the roles of IL-17A in AOM would increase understanding of the pathogenesis of AOM-related diseases and help in the development of effective therapeutic strategies.

## ACKNOWLEDGMENTS

This study is supported by National Natural Science Foundation grants of China (no. cscf81373151), Natural Science Foundation Project of CQCSTC (no. cstc2012jjA0035), and Scientific and Technological Research Program of Chongqing Municipal Education Commission grants of China (no. KJ130313).

We are grateful to Zhinan Yin from Nankai University and Richard A. Flavell from the Yale University School of Medicine for kindly providing the IL-17A KO mice. We thank Jun Wu from the University of South Carolina and Bruce Stevenson from Peking University for the critical reading and comments. We thank Zhiqiang Ding for the correction of the English usage of the manuscript.

We declare that we have no conflicts of interest.

## REFERENCES

1. Monasta L, Ronfani L, Marchetti F, Montico M, Vecchi Brumatti L, Bavcar A, Grasso D, Barbiero C, Tamburlini G. 2012. Burden of disease caused by otitis media: systematic review and global estimates. *PLoS One* 7: e36226. <http://dx.doi.org/10.1371/journal.pone.0036226>.
2. Bakaletz LO. 2010. Immunopathogenesis of polymicrobial otitis media. *J. Leukoc. Biol.* 87:213–222. <http://dx.doi.org/10.1189/jlb.0709518>.
3. Barkai G, Leibovitz E, Givon-Lavi N, Dagan R. 2009. Potential contribution by nontypable *Haemophilus influenzae* in protracted and recurrent acute otitis media. *Pediatr. Infect. Dis. J.* 28:466–471. <http://dx.doi.org/10.1097/INF.0b013e3181950c74>.
4. Cua DJ, Tato M. 2010. Innate IL-17-producing cells: the sentinels of the immune system. *Nat. Rev. Immunol.* 10:479–489. <http://dx.doi.org/10.1038/nri2800>.
5. Lin AM, Rubin CJ, Khandpur R, Wang JY, Riblett M, Yalavarthi S, Villanueva EC, Shah P, Kaplan MJ, Bruce AT. 2011. Mast cells and neutrophils release IL-17 through extracellular trap formation in psoriasis. *J. Immunol.* 187:490–500. <http://dx.doi.org/10.4049/jimmunol.1100123>.
6. Xu S, Cao X. 2010. Interleukin-17 and its expanding biological functions. *Cell Mol. Immunol.* 7:164–174. <http://dx.doi.org/10.1038/cmi.2010.21>.
7. Matsuzaki G, Umemura M. 2007. Interleukin-17 as an effector molecule of innate and acquired immunity against infections. *Microbiol. Immunol.* 51:1139–1147. <http://dx.doi.org/10.1111/j.1348-0421.2007.tb04008.x>.
8. Hamada S, Umemura M, Shiono T, Tanaka K, Yahagi A, Begum MD, Oshiro K, Okamoto Y, Watanabe H, Kawakami K, Roark C, Born WK, O'Brien R, Ikuta K, Ishikawa H, Nakae S, Iwakura Y, Ohta T, Matsuzaki G. 2008. IL-17A produced by  $\gamma\delta$  T cells plays a critical role in innate immunity against listeria monocytogenes infection in the live. *J. Immunol.* 181:3456–3463.
9. Schulz SM, Köhler G, Holscher C, Iwakura Y, Alber G. 2008. IL-17A is produced by Th17,  $\gamma\delta$  T cells and other CD4<sup>+</sup> lymphocytes during infection with *Salmonella enterica* serovar Enteritidis and has a mild effect in bacterial clearance. *Int. Immunol.* 20:1129–1138. <http://dx.doi.org/10.1093/intimm/dxn069>.
10. Zhang X, Majlessi L, Deriaud E, Leclerc C, Lo-Man R. 2009. Coactivation of Syk kinase and MyD88 adaptor protein pathways by bacteria promotes regulatory properties of neutrophils. *Immunity* 31:761–771. <http://dx.doi.org/10.1016/j.immuni.2009.09.016>.
11. McEllistrem MC, Adams JM, Patel K, Mendelsohn AB, Kaplan SL, Bradley JS, Schutze GE, Kim KS, Mason EO, Wald ER. 2005. Acute otitis media due to penicillin-nonsusceptible *Streptococcus pneumoniae* before

- and after the introduction of the pneumococcal conjugate vaccine. *Clin. Infect. Dis.* 40:1738–1744. <http://dx.doi.org/10.1086/429908>.
12. Tong HH, Li YX, Stahl GL, Thurman JM. 2010. Enhanced susceptibility to acute pneumococcal otitis media in mice deficient in complement C1qa, factor B, and factor B/C2. *Infect. Immun.* 78:976–983. <http://dx.doi.org/10.1128/IAI.01012-09>.
  13. MacArthur CJ, Hefeneider SH, Kempton JB, Parrish SK, McCoy SL, Trune DR. 2006. Evaluation of the mouse model for acute otitis media. *Hear. Res.* 219:12–23. <http://dx.doi.org/10.1016/j.heares.2006.05.012>.
  14. Long JP, Tong HH, Shannon PA, DeMaria TF. 2003. Differential expression of cytokine genes and inducible nitric oxide synthase induced by opacity phenotype variants of *Streptococcus pneumoniae* during acute otitis media in the rat. *Infect. Immun.* 71:5531–5540. <http://dx.doi.org/10.1128/IAI.71.10.5531-5540.2003>.
  15. Ferretti S, Bonneau O, Dubois GR, Jones CE, Trifilieff A. 2003. IL-17, produced by lymphocytes and neutrophils, is necessary for lipopolysaccharide-induced airway neutrophilia: IL-15 as a possible trigger. *J. Immunol.* 170:2106–2112.
  16. Werner JL, Gessner MA, Lilly LM, Nelson MP, Metz AE, Horn D, Dunaway CW, Deshane J, Chaplin DD, Weaver CT, Brown GD, Steele C. 2011. Neutrophils produce interleukin 17A (IL-17A) in a dectin-1- and IL-23-dependent manner during invasive fungal infection. *Infect. Immun.* 79:3966–3977. <http://dx.doi.org/10.1128/IAI.05493-11>.
  17. Korn T, Bettelli E, Oukka M, Kuchroo VK. 2009. IL-17 and Th17 Cells. *Annu. Rev. Immunol.* 27:485–517. <http://dx.doi.org/10.1146/annurev.immunol.021908.132710>.
  18. Nathan C. 2006. Neutrophils and immunity: challenges and opportunities. *Nat. Rev. Immunol.* 6:173–178. <http://dx.doi.org/10.1038/nri1785>.
  19. Garvy BA, Harmsen AG. 1996. The importance of neutrophils in resistance to pneumococcal pneumonia in adult and neonatal mice. *Inflammation* 20:499–512. <http://dx.doi.org/10.1007/BF01487042>.
  20. Nograles KE, Zaba LC, Guttman-Yassky E, Fuentes-Duculan J, Suárez-Fariñas M, Cardinale I, Khatcherian A, Gonzalez J, Pierson JC, White TR, Pensabene C, Coats I, Novitskaya I, Lowes MA, Krueger JG. 2008. Th17 cytokines interleukin (IL)-17 and IL-22 modulate distinct inflammatory and keratinocyte-response pathways. *Br. J. Dermatol.* 159:1092–1102. <http://dx.doi.org/10.1111/j.1365-2133.2008.08769.x>.
  21. Albanesi C, Scarponi C, Cavani A, Federici M, Nasorri F, Girolomoni G. 2000. Interleukin-17 is produced by both Th1 and Th2 lymphocytes, and modulates interferon-gamma- and interleukin-4-induced activation of human keratinocytes. *J. Investig. Dermatol.* 115:81–87. <http://dx.doi.org/10.1046/j.1523-1747.2000.00041.x>.
  22. Hoeve MA, Savage ND, de Boer T, Langenberg DM, de Waal Malefyt R, Ottenhoff TH, Verreck FA. 2006. Divergent effects of IL-12 and IL-23 on the production of IL-17 by human T cells. *Eur. J. Immunol.* 36:661–670. <http://dx.doi.org/10.1002/eji.200535239>.
  23. Nie H, Zheng Y, Li R, Guo TB, He D, Fang L, Liu X, Xiao L, Chen X, Wan B, Chin YE, Zhang JZ. 2013. Phosphorylation of FOXP3 controls regulatory T cell function and is inhibited by TNF- $\alpha$  in rheumatoid arthritis. *Nat. Med.* 19:322–328. <http://dx.doi.org/10.1038/nm.3085>.
  24. Dong C. 2008. TH17 cells in development: an updated view of their molecular identity and genetic programming. *Nat. Rev. Immunol.* 8:337–348. <http://dx.doi.org/10.1038/nri2295>.
  25. Langrish CL, Chen Y, Blumenschein WM, Mattson J, Basham B, Sedgwick JD, McClanahan T, Kastelein RA, Cua DJ. 2005. IL-23 drives a pathogenic T cell population that induces autoimmune inflammation. *J. Exp. Med.* 201:233–240. <http://dx.doi.org/10.1084/jem.20041257>.
  26. Grommes J, Soehnlein O. 2011. Contribution of neutrophils to acute lung injury. *Mol. Med.* 17:293–307. <http://dx.doi.org/10.2119/molmed.2010.00138>.
  27. Cara DC, Kaur J, Forster M, McCafferty DM, Kubes P. 2001. Role of p38 mitogen-activated protein kinase in chemokine-induced emigration and chemotaxis in vivo. *J. Immunol.* 167:6552–6558.
  28. Yang Z, Zhang X, Darrah PA, Mosser DM. 2010. The regulation of Th1 responses by the p38 MAPK. *J. Immunol.* 185:6205–6213. <http://dx.doi.org/10.4049/jimmunol.1000243>.
  29. Puddicombe SM, Davies DE. 2000. The role of MAP kinases in intracellular signal transduction in bronchial epithelium. *Clin. Exp. Allergy* 30:7–11. <http://dx.doi.org/10.1046/j.1365-2222.2000.00709.x>.
  30. Chen Y, Kijlstra A, Chen Y, Yang P. 2011. IL-17A stimulates the production of inflammatory mediators via Erk1/2, p38 MAPK, PI3K/Akt, and NF- $\kappa$ B pathways in ARPE-19 cells. *Mol. Vis.* 17:3072–3077.
  31. Laan M, Lötvall J, Chung KF, Lindén A. 2001. IL-17-induced cytokine release in human bronchial epithelial cells in vitro: role of mitogen-activated protein (MAP) kinases. *Br. J. Pharmacol.* 133:200–206. <http://dx.doi.org/10.1038/sj.bjp.0704063>.
  32. Kawaguchi M, Kokubu F, Kuga H, Matsukura S, Hoshino H, Ieki K, Imai T, Adachi M, Huang SK. 2001. Modulation of bronchial epithelial cells by IL-17. *J. Allergy Clin. Immunol.* 108:804–809. <http://dx.doi.org/10.1067/mai.2001.119027>.
  33. Mitroulis I, Kourtzelis I, Kambas K, Rafail S, Chrysanthopoulou A, Speletas M, Ritis K. 2010. Regulation of the autophagic machinery in human neutrophils. *Eur. J. Immunol.* 40:1461–1472. <http://dx.doi.org/10.1002/eji.200940025>.
  34. Zychlinsky A, Sansonetti P. 1997. Perspectives series: host/pathogen interactions. Apoptosis in bacterial pathogenesis. *J. Clin. Invest.* 100:493–495. <http://dx.doi.org/10.1172/JCI119557>.
  35. Hersh D, Monack DM, Smith MR, Ghori N, Falkow S, Zychlinsky A. 1999. The *Salmonella* invasin SipB induces macrophage apoptosis by binding to caspase-1. *Proc. Natl. Acad. Sci. U. S. A.* 96:2396–2401. <http://dx.doi.org/10.1073/pnas.96.5.2396>.
  36. Dockrell DH, Lee M, Lynch DH, Read RC. 2001. Immune-mediated phagocytosis and killing of *Streptococcus pneumoniae* are associated with direct and bystander macrophage apoptosis. *J. Infect. Dis.* 184:713–722. <http://dx.doi.org/10.1086/323084>.
  37. Dockrell DH, Marriott HM, Prince LR, Ridger VC, Ince PG, Hellewell PG, Whyte MK. 2003. Alveolar macrophage apoptosis contributes to pneumococcal clearance in a resolving model of pulmonary infection. *J. Immunol.* 171:5380–5388.
  38. Steinwede K, Henken S, Bohling J, Maus R, Ueberberg B, Brumshagen C, Brincks EL, Griffith TS, Welte T, Maus UA. 2012. TNF-related apoptosis-inducing ligand (TRAIL) exerts therapeutic efficacy for the treatment of pneumococcal pneumonia in mice. *J. Exp. Med.* 209:1937–1952. <http://dx.doi.org/10.1084/jem.20120983>.
  39. Ali F, Lee ME, Iannelli F, Pozzi G, Mitchell TJ, Read RC, Dockrell DH. 2003. *Streptococcus pneumoniae*-associated human macrophage apoptosis after bacterial internalization via complement and Fc $\gamma$  receptors correlates with intracellular bacterial load. *J. Infect. Dis.* 188:1119–1131. <http://dx.doi.org/10.1086/378675>.
  40. Serhan CN, Savill J. 2005. Resolution of inflammation: the beginning programs the end. *Nat. Immunol.* 6:1191–1197. <http://dx.doi.org/10.1038/ni1276>.
  41. Cai B, Chang SH, Becker EB, Bonni A, Xia Z. 2006. p38 MAP kinase mediates apoptosis through phosphorylation of BimEL at Ser-65. *J. Biol. Chem.* 281:25215–25222. <http://dx.doi.org/10.1074/jbc.M512627200>.
  42. Boronkai A, Belyei S, Szigeti A, Pozsgai E, Bogнар Z, Sumegi B, Gallyas F, Jr. 2009. Potentiation of paclitaxel-induced apoptosis by galectin-13 overexpression via activation of Ask-1-p38-MAP kinase and JNK/SAPK pathways and suppression of Akt and ERK1/2 activation in U-937 human macrophage cells. *Eur. J. Cell Biol.* 88:753–763. <http://dx.doi.org/10.1016/j.ejcb.2009.07.005>.